

# Deletion mutagenesis as a test of evolutionary relatedness of indoleglycerol phosphate synthase with other TIM barrel enzymes

Catherine Stehlin<sup>a</sup>, Anke Dahm<sup>b</sup>, Kasper Kirschner<sup>b,\*</sup>

<sup>a</sup>Department of Chemistry, University of Minnesota, Minneapolis MN 55455, USA

<sup>b</sup>Department of Biophysical Chemistry, Biozentrum of the University, CH 4056 Basel, Switzerland

Received 14 January 1997

**Abstract** The role of the extra helix  $\alpha_0$  in the N-terminal extension of the eight-fold  $\beta\alpha$  barrel of indoleglycerol phosphate synthase was probed by point mutation and truncation. Replacing invariant leucine 5 by valine of the enzyme from *Escherichia coli* affected neither  $k_{\text{cat}}$  nor  $K_M$ , but deletion of 8 N-terminal residues decreased solubility strongly. The similarly truncated variant from the hyperthermophile *Sulfolobus solfataricus* was soluble, and had the same  $k_{\text{cat}}$  value as the wild-type protein but a 220-fold greater  $K_M$  value. These results suggest that the N-terminal portion of helix  $\alpha_0$  provides for strong binding of the substrate, but is not essential for stabilizing the bound transition state. Thus, three enzymes of tryptophan biosynthesis operate essentially as canonical eight-fold  $\beta\alpha$  barrels, as required for their divergent evolution.

© 1997 Federation of European Biochemical Societies.

**Key words:** Protein evolution; Protein engineering; Thermostability; TIM barrel protein; Indoleglycerol phosphate synthase

## 1. Introduction

Proteins with the eight-fold  $\beta\alpha$  ( $8\beta\alpha$  or TIM) barrel structure are a common choice of scaffold for positioning residues of enzymatic active sites [1]. The interior of the  $8\beta\alpha$  fold consists of 8 parallel  $\beta$  strands that form a central barrel-shaped  $\beta$  sheet. The  $\beta$  strands are connected by 8  $\alpha$  helices that cover the  $\beta$  barrel on the outside. Over 30 different enzymes are currently known to possess the  $8\beta\alpha$  barrel fold [1], and it is possible that several subfamilies of this fold have each arisen by divergent evolution from a single ancestor [2]. The assignment to a particular subfamily has been based on the similarity of the elliptical barrel cross-section, the location of inserts in particular loops, or both.

One such subfamily comprises the prototypical triose-phosphate isomerase (TIM [3]), and three consecutively operating enzymes from the pathway of biosynthesis of tryptophan [1,4]. These are phosphoribosyl anthranilate isomerase (PRAI, [5,6]), indoleglycerol phosphate synthase (IGPS, [5,7]) and the  $\alpha$  subunit of tryptophan synthase [8]. Each of the three enzymes is in principle a stable and active monomer [6–9]. The substrates are similar in having an aromatic ring connected to

phosphate by an hydrophilic linker. The subdomains that bind the phosphate moieties of the respective substrates of each enzyme are structurally very similar [4]. Moreover, it is likely that each reaction is catalyzed by the concerted action of a general acid and a general base [10], but detailed data on the catalytic mechanism are available only for the  $\alpha$  subunit of tryptophan synthase [8].

PRAI has the canonical  $8\beta\alpha$  fold such that it has no extensions of the sequence at the N- and C-termini [5]. The short N-terminal extension that is observed with some forms of the  $\alpha$  subunit of tryptophan synthase is not essential for its stability and function [11,12]. In contrast, IGPS possesses an additional helix  $\alpha_0$  at the beginning of a 50 residue long N-terminal extension [5,7]. It forms one wall of the active site at the C-terminal end of the central  $\beta$  barrel (Fig. 1A,B), and contains a single invariant residue, leucine 5 [11]. According to the hypothesis of divergent evolution [13], IGPS should be active as a canonical  $8\beta\alpha$  fold. Because the N-terminal extension does not fit in this hypothesis, we asked whether the invariant helix  $\alpha_0$  of IGPS is essential for its catalytic function.

Here we used protein engineering and enzyme kinetics to probe the role of the extra helix  $\alpha_0$  of the recombinant monofunctional IGPS domain from *Escherichia coli* (eIGPS [6]) by replacing the invariant leucine residue in the first turn by valine as well as by deleting the N-terminal portion of the helix  $\alpha_0$ . Because the deletion destabilizes eIGPS, the same deletions were constructed in both the bifunctional enzyme eIGPS-PRAI and in the thermostable, monofunctional IGPS from *Sulfolobus solfataricus* (sIGPS [7,9]). Deletion of the N-terminal portion of the extra helix  $\alpha_0$  increases  $K_M$  but does not affect  $k_{\text{cat}}$ .

## 2. Materials and methods

### 2.1. Bacterial strains and vectors

The source of the *etpC* gene for the monofunctional, monomeric eIGPS domain (IGPS[1–259]) was the plasmid pMc2.C [6], a derivative of pMc5-10 [14]. Selection strain *E. coli* WK6 mutS [14] was provided by Dr. Hans-Joachim Fritz, and expression strain *E. coli* W3110  $\Delta trpEA2$  (*tna2*, *trpR*) as well as the plasmid pWS1 [15] as the source of the *trpC(F)* gene by Dr. Charles Yanofsky. Dr. Dieter Stüber donated the expression vector pDS56/RBSII/*SphI* [16].

### 2.2. Mutagenesis procedures

Standard protocols [17] were followed for modifying DNA. Double-stranded DNA for large-scale preparation was isolated with the Qiagen purification kit according to the manufacturer's instructions. Single-stranded DNA was produced by infection with the helper phage M13 K07 (Pharmacia), and purified according to the manufacturer's instructions. The sequence of each mutant was verified by sequencing the entire mutant gene [18].

The L5V mutation was introduced into the *trpC* gene of *E. coli* (*etpC*) contained in the vector pMc2.C. The gapped duplex method

\*Corresponding author. Biozentrum der Universität Basel, Klingelbergstrasse 70, CH 4056 Basel, Switzerland.  
Fax: (41) (61) 267 2189.

**Abbreviations:** DTE, dithioerythritol; HEPPS, *N*-(2-hydroxyethyl)piperazine *N'*-(3-propanesulfonic acid); GdmCl, guanidinium chloride; PMSF, phenylmethyl sulfonyl fluoride; CdRP, 1-(*o*-carboxyphenylamino)-1-deoxyribose 5-phosphate; IGP, indoleglycerol phosphate; IGPS, indoleglycerol phosphate synthase; PRAI, phosphoribosyl anthranilate isomerase; eIGPS-PRAI, bifunctional enzyme from *E. coli*

[19], was used with the synthetic oligonucleotide 5'-TGC GAC GAT TTT CGC GAC AAC GGT TTG CAT CAT-3'. It is complementary to the first 10 codons of *etpC*, except for those of L5 and A6. These replacements introduced the mutation L5V, a silent codon change for A6, and an additional *NruI* site (underlined).

eL5V was first expressed from the resulting vector pMc2.CL5V in *E. coli* W3110  $\Delta$ trpEA2. To boost expression, it was desirable to subclone the *trpC* genes into the expression vector pDS56/RBSII/*SphI* [16]. To this end a new *SphI* site was introduced into the second methionine codon of *etpC*, using the synthetic oligonucleotide 5'-C GGT TTG CAT GCT TTA CCC TCG-3'. It is complementary to the first four codons of *etpC*, but the first methionine codon is changed to AGC for serine, and is therefore not expressed. Translation of *etpC*(F) appears to initiate at the second AUG codon [20]. The resulting *SphI*-*HindIII* fragment that contains the coding region of eL5V was then inserted into pDS56/RBSII/*SphI*. The same *SphI* site was also inserted into the wild-type *etpC* gene for overexpression from the same vector in the same strain of *E. coli*.

The vector pWS1 [15], which contains the *etpC*(F)BA genes, was the template for deleting the first 8 codons of *etpC*(F), using the polymerase chain reaction (PCR). Primer sequences were (a) 5'-A AGC ATG CTT GAC AAG GCG ATT TGG GTA G-3', in which codons 2–9 of the *etpC*(F) gene are deleted. This primer introduces the same new *SphI* site as used for the coding sequence of eL5V above, as well as the codon change for A10L. Primer (b) 3'-CTT CGA AAA CAG TCA CGC GT-5', which is complementary to the 5'-terminus of the coding strand of *trpB*, introduces a new *HindIII* site. The amplified gene of e $\Delta$ (2–9) IGPS-PRAI was inserted as *SphI*/*HindIII* fragment into the expression vector pDS56/RBSII/*SphI* and expressed as described above.

Codons 2–9 of the *trpC* gene of *S. solfataricus* (*strpC*) were deleted from the vector pDS SS-1 [7] by PCR, using the following two synthetic oligonucleotides as primers: (a) 5'-AA AGC ATG CGA GAC GTC GTA CAA TTA TC-3', which deleted codons 2–9 and replaced the codon of K10 by one for R; (b) 3'-TTC TAA TTT CTT AAA TAT GAT ATC GAC GTC AAA-5', which introduces a new *PstI* site [7]. The gene of s $\Delta$ (2–9) was expressed as described [7].

### 2.3. Protein purification

sIGPS wild-type [21] and s $\Delta$ (2–9) were produced as recombinant proteins in *E. coli* and purified from the soluble fraction of cell homogenates as described [7]. The yields of purified proteins (mg protein per g of wet cell paste) were: sIGPS, 1.5; s $\Delta$ (2–9), 0.31. Wild-type eIGPS-PRAI was purified as described [6]. Because the expression of the genes of eIGPS (IGPS[1–259], [6]), eL5V and e $\Delta$ (2–9)-PRAI employed the efficient expression vector pDS56/RBSII/*SphI* [16], these proteins were recovered from the insoluble fraction of cell homogenates, and were already about 90% pure. The purification of eL5V and s $\Delta$ (2–9) was monitored by measuring the IGPS reaction [6,7], that of e $\Delta$ (2–9)-PRAI by the PRAI reaction [6].

Cells were sonicated at 0°C in 0.1 M Tris-HCl buffer (pH 8.0) containing 6 mM MgCl<sub>2</sub>, 2 mM DTE, 0.1 mM PMSF and 50 units of the non-specific endonuclease benzonase (Merck; buffer A). All further steps were performed at 4°C. The pellet obtained after centrifugation was washed twice with buffer A, once with buffer A containing both 0.1% (v/v) Triton X-100 and 0.5 M NaCl, and finally twice with 0.05 M K phosphate (pH 7.5) containing 2 mM EDTA, 2 mM DTE, 0.1 mM PMSF and 0.3 M NaCl (buffer B). The washed pellet (1 g) was dissolved in 25 ml of buffer B containing 6 M GdmCl at 25°C. The clarified supernatant was diluted 25-fold with buffer B (pH 8.0, 4°C) containing 3 M GdmCl, and dialyzed at 4°C against several changes of 4 l each of buffer B, with stepwise decrease of pH in 0.5 pH units from 8.0 to 7.0. Precipitate was removed by centrifugation. The supernatant was concentrated with PM-10 membranes (Amicon) and subjected to gel filtration on a column (2.5×90 cm, 440 ml volume) of Sephacryl S-200 (Pharmacia) in buffer B (pH 7.5) supplemented with 2 mM EDTA, 2 mM DTE and 0.3 M NaCl. In the case of e $\Delta$ (2–9)-PRAI, the gel filtration step was replaced by ion exchange chromatography on a column (3 cm×25 cm, 270 ml volume) of DEAE-Sephacrose fast flow (Pharmacia). The column was equilibrated with 10 mM K phosphate (pH 7.5) supplemented with 2 mM EDTA and 2 mM DTE. The protein was eluted with a linear gradient of 1.2 l increasing from 40 to 500 mM K phosphate. Fractions with the highest PRAI specific activity were pooled and concentrated as above. The yields of concentrated and clarified proteins (mg protein

per g of wet cell paste) were: eIGPS, 16.5; eL5V, 9.0; e $\Delta$ (2–9), 0.04; e $\Delta$ (2–9)-PRAI, 0.25.

### 2.4. Analytical methods

Protein preparations were tested for homogeneity by SDS-PAGE [22]. Protein concentration was determined spectrophotometrically with the following values of  $A_{280}^{0.1\%}$  (cm<sup>2</sup> mg<sup>−1</sup>): eIGPS-PRAI (and e $\Delta$ (2–9)-PRAI), 0.84 [6]; eIGPS (and e $\Delta$ (2–9)), 0.81 [6]; sIGPS, 0.606 [7]; s $\Delta$ (2–9), 0.60 (calculated). During purification, protein concentrations were estimated with the Bradford assay [23], with bovine serum albumin as standard. Molecular masses were measured by analytical gel filtration experiments at 25°C in 0.05 M K phosphate (pH 7.5) supplemented with 2 mM EDTA and 2 mM DTE. The column of Superose 12 (1×30 cm, Pharmacia) was calibrated using the following standard proteins (molecular masses in kDa): cytochrome *c* (12.4), eIGPS (28.9), ovalbumin (43.0), eIGPS-PRAI (49.5), bovine serum albumin (66.3), and phosphorylase *b* (194.8). PRAI activity was assayed at 25°C in 0.05 M Tris-HCl (pH 7.5) containing 4 mM K<sub>2</sub>MgEDTA and 2 mM DTE by monitoring the decrease of substrate (PRA) fluorescence as described [24]. IGPS activity was assayed at 25°C in the same buffer by monitoring the increase of product (IGP) fluorescence [25]. Both sIGPS and s $\Delta$ (2–9) were assayed at 25°C in 0.05 M HEPES buffer (pH 7.5) supplemented with 4 mM EDTA [7]. Initial velocities as function of substrate concentration as well as fitting of entire progress curves were used to determine values of  $k_{cat}$  and  $K_M$  [6,24].

## 3. Results and discussion

Fig. 1A presents a side view of the eIGPS domain [5] to illustrate that the first turn of the extra helix  $\alpha_0$  forms one of the four walls encasing the active site. The loops  $\beta_1\alpha_1$ ,  $\beta_2\alpha_2$  and  $\beta_5\alpha_6$  furnish the other three walls (Fig. 1B). The first 22 residues of eIGPS, including helix  $\alpha_0$ , are fixed to the surface of the 8 $\beta\alpha$  barrel by one hydrogen bond (R19 to Y121 in  $\alpha_3$ ) and 4 salt bridges: D11 to K91 in  $\beta_1\alpha_1$ , K12 to both D89 in  $\beta_2\alpha_2$  and D115 in  $\beta_3\alpha_3$  as well as K20 to D119 in  $\beta_3\alpha_3$  [5]. As judged by the main chain temperature factors of eIGPS [5], the first two turns of  $\alpha_0$  (V<sub>4</sub>–D<sub>11</sub>) are tightly fixed to the body of the protein and contain residue L5, which is the only invariant residue in the N-terminal extension. Fig. 1B shows that residue L5, together with the invariant residues P59 ( $\beta_1\alpha_1$ ), F93 ( $\beta_2\alpha_2$ ), F116 ( $\beta_3\alpha_3$ ) and L188 ( $\beta_6\alpha_6$ ), forms an hydrophobic pocket at the top of the active site [5]. It is likely to bind the benzoic acid moiety of the substrate 1-(*o*-carboxyphenylamino)-1-deoxyribulose 5-phosphate (CdRP) shown in Fig. 2. We therefore decided to probe the role of L5 and the first turn of the helix  $\alpha_0$  by measuring the enzyme kinetic constants of the following mutants of eIGPS, which are defined in Fig. 3: Conservative replacement of the invariant residue L5 by valine (eL5V), and deletion of 8 residues at the N-terminus (e $\Delta$ (2–9)).

The point mutant eL5V was introduced into the *etpC* gene of *E. coli* (severed from its natural downstream fusion partner *etpF*, [6]) by means of the gapped duplex method [14]. This construct was inserted into an inducible expression vector [16] and expressed in a strain of *E. coli* that lacks the entire *trp* operon [15]. Similar to the monomeric eIGPS domain [6], the recombinant variant was found predominantly in the insoluble fraction of the cell homogenate. It was therefore solubilized in buffer containing 6 M guanidinium chloride (GdmCl), refolded by dialysis against buffer and purified by gel filtration.

The enzyme kinetic constants of the essentially pure eL5V are presented in Table 1. The values of  $k_{cat}$ ,  $K_M^{CdRP}$  and the efficiency parameter  $k_{cat}/K_M^{CdRP}$  differ only marginally from

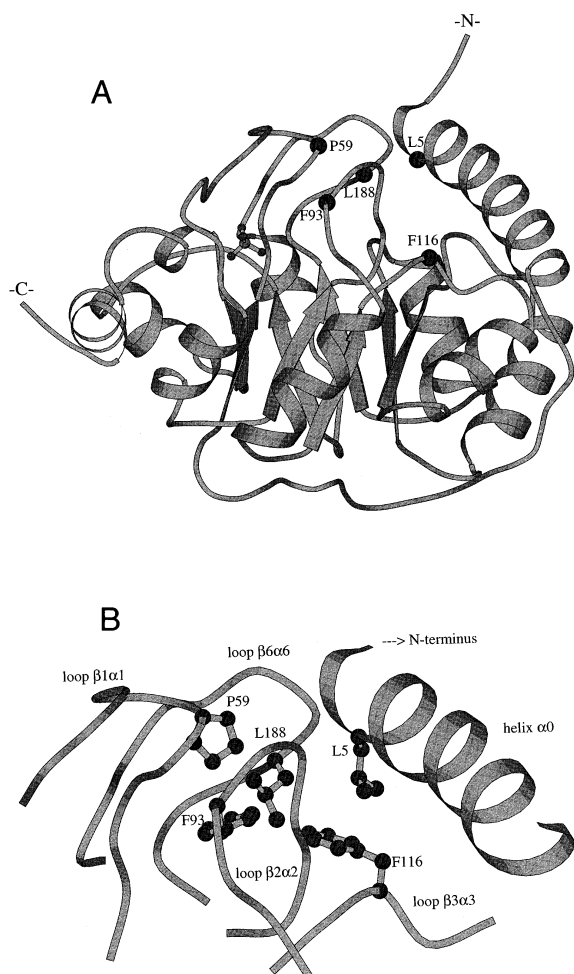


Fig. 1. (A) Ribbon representation of the indoleglycerol phosphate synthase domain from *E. coli* (eIGPS [5]). Dots label the  $\alpha$  positions of the invariant residues located on the segments of the folded protein indicated in parentheses: L5 ( $\alpha_0$ ), P59 ( $\beta_1\alpha_1$ ), F93 ( $\beta_2\alpha_2$ ), F116 ( $\beta_3\alpha_3$ ) and L188 ( $\beta_6\alpha_6$ ), which line the hydrophobic pocket. (B) Enlarged view of the hydrophobic pocket. Helix  $\alpha_0$  and the relevant loops between strands  $\beta_i$  and helices  $\alpha_i$  ( $\beta_i\alpha_i$ ) are labelled and the side chains of L5, P59, F93, F116 and L188 are presented as ball-and-stick models.

those of the wild-type eIGPS. However, a significant difference in solubility was observed when both the wild-type and mutant *etp* genes were expressed constitutively with the mutagenesis and expression vector pMc2.C [6]. As judged by polyacrylamide gel electrophoresis in the presence of SDS (SDS-PAGE), eIGPS was distributed evenly between the pellet and supernatant of cell homogenates, whereas most of eL5V was deposited in the pellet (data not shown). Moreover, the maximal concentration of purified soluble eL5V attainable before the onset of aggregation (0.2 mg protein/ml) is much lower than that of eIGPS (2–10 mg/ml [6,26]). We conclude that the replacement eL5V shifts the equilibrium of the monomeric protein between the stable native and a destabilized, aggregation-prone conformation, in favour of the latter. Since the N-terminal residues of eIGPS (M1 and Q2, cf. Figs. 1 and 3) are fixed by crystal lattice contacts [5] and are likely to be mobile in the dissolved molecule, it appears that L5 provides an important anchor point for the N-terminus of helix  $\alpha_0$ . All of the hydrogen bonds and salt bridges fixing helix  $\alpha_0$  to the

surface of the  $8\beta\alpha$  barrel (see above) can still be formed. Nevertheless, the conservative replacement eL5V seems to weaken this interaction sufficiently to promote aggregation. Because eL5V is as active as wild-type eIGPS, we undertook the more drastic modification of deleting the first two turns of helix  $\alpha_0$  of eIGPS.

Using PCR mutagenesis, we removed 8 codons of the *etpC* gene between M<sub>1</sub> and D<sub>11</sub> (Fig. 3) and replaced residue A10 (A10L), for technical reasons. The truncated *etpC* gene was inserted into the same expression vector as used for eL5V, and expressed and purified as before. The tendency of e $\Delta(2-9)$  to aggregate was even stronger than that of eL5V, so that its kinetic constants could not be determined. We therefore constructed the deletion e $\Delta(2-9)$  in the naturally bifunctional *etpC(F)* gene. We reasoned that this measure would stabilize the deletion mutant of the eIGPS domain. Indeed, the resulting protein (e $\Delta(2-9)$ -PRAI) was more soluble than e $\Delta(2-9)$ . Nevertheless, its catalytic activity was so reduced by comparison to eIGPS that we could only determine the efficiency parameter  $k_{\text{cat}}/K_M^{\text{CdRP}}$  from the initial slope of the plot of initial velocity versus substrate concentration (Table 1). Analytical gel filtration on a Superose 12 column showed that soluble e $\Delta(2-9)$ -PRAI obtained by concentrating the pooled fractions of the protein eluted from DEAE-Sephacel consisted of only 17% monomer (Fig. 4A). The major fraction eluted in the range of apparent dimers and hexamers. In contrast, the wild-type eIGPS-PRAI eluted as a monomer with less than 10% apparent dimers (Fig. 4B). Controls showed that the  $k_{\text{cat}}$  and  $K_M^{\text{PRA}}$  values of the PRAI reaction catalyzed by the ePRAI domain of e $\Delta(2-9)$ -PRAI were identical to those observed for the wild-type ([6], data not shown). This observation indicates that the ePRAI domain is correctly folded and fully accessible to the substrate PRA, even in the apparent dimers and hexamers of e $\Delta(2-9)$ -PRAI. To circumvent the problems arising from the marginal stability of the deletion mutants of eIGPS and eIGPS-PRAI, we turned to the recently available naturally monomeric IGPS from the hyperthermophile *S. solfataricus* (sIGPS, [7,9,21]) and constructed the  $\Delta(2-9)$  deletion in a thermostable background.

The N-terminal sequences of eIGPS and sIGPS have been aligned (Fig. 3) on the basis of superimposed X-ray structures [7]. sIGPS is four residues longer than eIGPS, and invariant residue L9 of sIGPS is structurally equivalent to L5 of eIGPS. Using PCR mutagenesis we removed 8 codons of the *etpC* gene of *S. solfataricus* between M1 and K10, including those of both L9 and W8, the single W residue contained in sIGPS

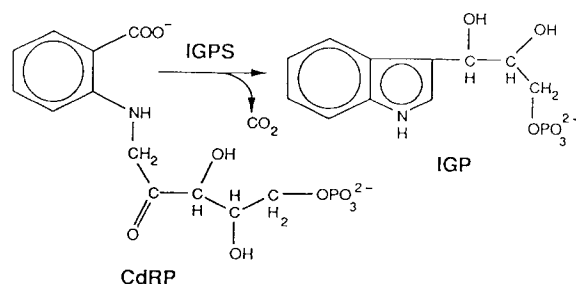


Fig. 2. The substrate and product of the reaction catalyzed by indoleglycerol phosphate synthase (IGPS) both possess hydrophobic aromatic moieties connected by an hydrophilic linker to phosphate. CdRP, 1-(O-carboxyphenylamino)-1-deoxyribulose 5-phosphate; IGP, indoleglycerol phosphate.

[21]. Residue K10 was replaced conservatively (K10R), for technical reasons. Helix  $\alpha_0$  of sIGPS is shorter (11 residues) than helix  $\alpha_0$  of eIGPS (18 residues, Fig. 3), and the deletion s $\Delta$ (2–9) removes only the first turn of helix  $\alpha_0$ .

The truncated *strpC* gene was inserted into the same expression vector that was used for the production of sIGPS [7], and expressed as described. s $\Delta$ (2–9) is a stable protein, and was purified exactly as described for sIGPS [7]. sIGPS excited at 280 nm fluoresces maximally at 331 nm (data not shown), reflecting contributions from tyrosine residues and the single tryptophan residue W8 [21]. The fluorescence emission maximum of s $\Delta$ (2–9) was at 304 nm as expected for a protein containing tyrosine and no tryptophan residues. In contrast to e $\Delta$ (2–9), s $\Delta$ (2–9) displayed no tendency to aggregate, even at high concentrations. In analytical gel filtration experiments it eluted as a single peak in the expected monomer position (data not shown). These data demonstrate the usefulness of thermostable orthologous enzymes for mutations that otherwise destabilize thermolabile enzymes.

sIGPS is much less active at 25°C than eIGPS (Table 1; [7]). However, in contrast to e $\Delta$ (2–9)-PRAI, it was possible to measure independently both  $k_{cat}$  and  $K_M^{CdRP}$  of s $\Delta$ (2–9). Table 1 shows that the deletion of the first turn of helix  $\alpha_0$  of sIGPS increases  $K_M^{CdRP}$  220-fold without changing the value of  $k_{cat}$  significantly. The ratio of mutant to wild-type  $k_{cat}/K_M^{CdRP}$  values is 13-fold larger than that of e $\Delta$ (2–9)-PRAI. This observation correlates with the approx. 1:6 distribution of the protein between monomers and oligomers (Fig. 4A,B). Intermolecular interactions leading to oligomerization of eIGPS are caused by deletion of the N-terminal portion of helix  $\alpha_0$ , which forms one wall of the active site (Fig. 1A,B). The simplest model for oligomerization is that deletion removes an important anchor of helix  $\alpha_0$  to the active site, so that the remainder of helix  $\alpha_0$  has the choice to interact intrasubunit as well as intermolecularly. Presumably the IGPS active sites are blocked in the oligomers, and only the monomer form of e $\Delta$ (2–9)-PRAI is active in the IGPS reaction. The observation (see above) that the PRAI activity of e $\Delta$ (2–9)-PRAI is not affected by oligomerization suggests that the PRAI domain is not directly involved in this process. Assuming that the preparation of e $\Delta$ (2–9) PRAI contains 17% active monomers (Fig. 4A), the corrected value of  $k_{cat}/K_M^{CdRP}$  is  $0.017 \mu M^{-1} s^{-1}$  (Table 1). The ratio of mutant to wild-type  $k_{cat}/K_M^{CdRP}$  values is now similar to that of sIGPS and s $\Delta$ (2–9).

Previous work [6] has shown that changes in  $K_M^{CdRP}$  reflect

e $\Delta$ (2–9)	M - - - - - * L D K A I W V E A R K Q...
eL5V	M Q T V V A K I V A D K A I W V E A R K Q...
eIGPS	1                                   10                                   20 M Q T V L A K I V A D K A I W V E A R K Q...
sIGPS	1                                   10                                   20 M P R Y L K G W L K D V V Q L S L R R P S F R A S...
s $\Delta$ (2–9)	1                                   * M - - - - - R D V V Q L S L R R P S F R A S...

Fig. 3. Indoleglycerol phosphate synthase from *E. coli* and *S. solfataricus*: Sequence alignment, variants and definition of abbreviations. Alignment of N-terminal sequences of IGPS from *E. coli* (eIGPS) and *S. solfataricus* (sIGPS) based on superposition of X-ray structures [7]. Residues of respective helix  $\alpha_0$  underlined. (\*) Point mutants. (–) Deleted residues. eL5V, point mutant of eIGPS; e $\Delta$ (2–9), deletion mutant of eIGPS and eIGPS-PRAI; s $\Delta$ (2–9), deletion mutant of sIGPS. See text for details.

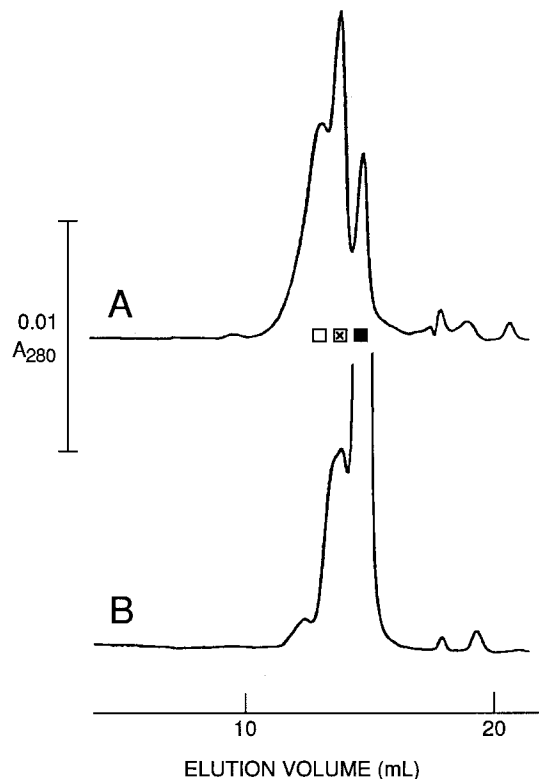


Fig. 4. Deletion of the first 8 residues of eIGPS-PRAI promotes specific oligomerization. Analytical gel chromatography at 25°C on Superose 12 column in buffer (pH 7.5). Absorbance at 280 nm recorded as a function of the elution volume. (■) Monomer; (⊠) dimer, (□) hexamer. (A) 25  $\mu g$  e $\Delta$ (2–9)-PRAI purified by anion exchange chromatography on DEAE-Sepharose and concentrated by ultrafiltration. The monomer peak amounts to 17% of the total peak area. (B) 50  $\mu g$  wild-type eIGPS-PRAI.

directly changes in  $K_d^{CdRP}$ , the thermodynamic dissociation constant of the enzyme-substrate complex. Under these special circumstances it is clear that the strong decrease of catalytic efficiency (measured by  $k_{cat}/K_M^{CdRP} \approx k_{cat}/K_d^{CdRP}$ ) is mainly due to a dramatic decrease of affinity for the substrate ( $1/K_d^{CdRP}$ ). In contrast, the constancy of  $k_{cat}$  indicates that the bound transition state of the IGPS reaction is stabilized to the same degree with respect to the bound substrate in both the wild-type and the deletion mutant. Because that portion of the N-terminal extension of IGPS that is most closely associated with the active site (Fig. 1B) is not essential for the intrinsic

Table 1  
Enzyme kinetic constants of indoleglycerol phosphate synthase and its variants at pH 7.5 and 25°C

Protein <sup>a</sup>	$k_{cat}$ ( $s^{-1}$ )	$K_M^{CdRP}$ ( $\mu M$ )	$k_{cat}/K_M^{CdRP}$ ( $\mu M^{-1} s^{-1}$ )	Ratio <sup>b</sup>
eIGPS	2.2	0.34	6.5	1.0
eL5V	2.0	0.21	9.6	1.47
e $\Delta$ (2–9)-PRAI	–	–	0.003 <sup>c</sup>	$4.5 \times 10^{-4}$
	–	–	0.017 <sup>d</sup>	$2.6 \times 10^{-3}$ <sup>d</sup>
sIGPS	0.033	0.045	0.73	1.0
s $\Delta$ (2–9)	0.041	9.9	0.0042	$5.8 \times 10^{-3}$

<sup>a</sup>Abbreviations given in Fig. 3.

<sup>b</sup> $(k_{cat}/K_M^{CdRP})_{var}/(k_{cat}/K_M^{CdRP})_{wt}$ .

<sup>c</sup>Initial slope of  $v_i$  vs.  $[CdRP]$  plot, see text.

<sup>d</sup>Calculated values, assuming that only monomers (17%) are enzymically active (Fig. 4A).

catalytic function of IGPS, it is possible that the entire extra helix  $\alpha_0$  may be expendable. That is to say that the intrinsic function of IGPS is sustained by the canonical  $8\beta\alpha$  barrel fold, which is in keeping with the hypothesis that the three  $8\beta\alpha$  barrel enzymes of tryptophan biosynthesis (PRAI, IGPS and the  $\alpha$  subunit of tryptophan synthase) have arisen by divergent evolution from a common ancestor [1,2,13]. The extension may have been recruited at a later stage to improve the affinity of IGPS for its substrate. Deletion of the entire helix  $\alpha_0$  is underway to provide further support for this hypothesis.

**Acknowledgements:** The authors thank A. Löschmann and H. Szadkowski for superb assistance, Drs. H.-J. Fritz, D. Stüber and C. Yanofsky for plasmids and bacterial strains, Dr. P. Jenö and Dr. W. Zürcher for synthetic oligonucleotides, as well as Dr. M. Hennig and T. Knöchel for preparing Fig. 1. Thanks are due to Drs. R. Sterner and C. Yanofsky for discussions. This work was supported by the Swiss National Science Foundation grant 31-32369.91.

## References

- [1] Reardon, D.R. and Farber, G.K. (1995) *FASEB J.* 9, 497–503.
- [2] Farber, G.K. and Petsko, G.A. (1990) *Trends Biochem. Sci.* 15, 228–234.
- [3] Banner, D.W., Bloomer, A.C., Petsko, G.A., Phillips, D.C., Pogson, C.I., Wilson, I.A., Corran, P.H., Furth, A.J., Milman, J.D., Offord, R.E., Priddle, J.D. and Waley, S.G. (1975) *Nature* 255, 609–614.
- [4] Wilmanns, M., Hyde, C.C., Davies, D.R., Kirschner, K. and Jansonius, J.N. (1991) *Biochemistry* 30, 9161–9169.
- [5] Wilmanns, M., Priestle, J.P., Niermann, T. and Jansonius, J.N. (1992) *J. Mol. Biol.* 223, 477–507.
- [6] Eberhard, M., Tsai-Pflugfelder, M., Bolewska, K., Hommel, U. and Kirschner, K. (1995) *Biochemistry* 34, 5419–5428.
- [7] Hennig, M., Darimont, B., Sterner, R., Kirschner, K. and Jansonius, J.N. (1995) *Structure* 3, 1295–1306.
- [8] Miles, E.W. (1991) *Adv. Enzymol. Relat. Areas Mol. Biol.* 64, 93–172.
- [9] Andreotti, G., Tutino, M.L., Sannia, G., Marino, G. and Cubellis, M.V. (1994) *Biochim. Biophys. Acta* 1208, 310–315.
- [10] Bentley, R. (1990) *Crit. Rev. Biochem. Mol. Biol.* 25, 307–384.
- [11] Sterner, R., Dahm, A., Darimont, B., Ivans, A., Liebl, W. and Kirschner, K. (1995) *EMBO J.* 14, 4395–4402.
- [12] Yee, M.C., Horn, V. and Yanofsky, C. (1996) *J. Biol. Chem.* 271, 14754–14763.
- [13] Jensen, R.A. (1992) in: *The Evolution of Metabolic Function* (Mortlock, R.P. ed.) pp. 205–336, Telford Press, West Caldwell, NJ.
- [14] Stanssens, P., Opsomer, C., McKeown, M.Y., Kramer, W., Zabeau, M. and Fritz, H.J. (1989) *Nucl. Acids. Res.* 17, 4441–4454.
- [15] Schneider, W.P. and Yanofsky, C. (1981) *Proc. Natl. Acad. Sci. USA* 78, 2169–2173.
- [16] Certa, U., Bannwarth, W., Stueber, D., Gentz, R., Lanzer, M., Le Brice, S., Guillot, F., Wendler, I., Hunsmann, G., Bujard, H. and Mous, J. (1986) *EMBO J.* 5, 3051–3056.
- [17] Sambrook, J., Fritsch, E.F. and Maniatis, T. (1989) *Molecular Cloning: A Laboratory Manual*, Cold Spring Harbor Laboratory, Cold Spring Harbor, NY.
- [18] Sanger, F., Nicklen, S. and Coulson, A.R. (1977) *Proc. Natl. Acad. Sci. USA* 74, 5463–5467.
- [19] Kramer, W. and Fritz, H.-J. (1987) *Methods Enzymol.* 154, 350–367.
- [20] Christie, G.E. and Platt, T. (1980) *J. Mol. Biol.* 142, 519–530.
- [21] Tutino, M.L., Scarano, G., Marino, G., Sannia, G. and Cubellis, M.V. (1993) *J. Bacteriol.* 175, 299–302.
- [22] Studier, F.W. (1973) *J. Mol. Biol.* 79, 237–248.
- [23] Bradford, M.M. (1976) *Anal. Biochem.* 72, 248–254.
- [24] Hommel, U., Eberhard, M. and Kirschner, K. (1995) *Biochemistry* 34, 5429–5439.
- [25] Hankins, C.N., Lagen, M. and Mills, S.E. (1975) *Anal. Biochem.* 69, 510–517.
- [26] Wilmanns, M., Schlagenhaut, E., Fol, B. and Jansonius, J.N. (1990) *Protein Eng.* 3, 173–180.